Eur Biophys J (2009) 38:523–532
DOI 10.1007/s00249-009-0402-8

ORIGINAL PAPER

Roles of surface residues of intracellular domains of heag potassium channels

Louisa Stevens · Min Ju · Dennis Wray

Received: 25 September 2008 / Revised: 12 December 2008 / Accepted: 19 December 2008 / Published online: 27 January 2009

Abstract Ether-a-go-go potassium channels have large intracellular regions containing 'Per-Ant-Sim' (PAS) and cyclic nucleotide binding (cNBD) domains at the N- and C-termini, respectively. In heag1 and heag2 channels, recent studies have suggested that the N- and C-terminal domains interact, and affect activation properties. Here, we have studied the effect of mutations of residues on the surfaces of PAS and cNBD domains. For this, we introduced alanine and lysine mutations in heag1 channels, and recorded currents by two-electrode voltage clamp. In both the PAS domain and the cNBD domain, contiguous areas of conserved residues on the surfaces of these domains were found which affected the activation kinetics of the channel. Next, we investigated possible effects of mutations on domain interactions of PAS and cNBD proteins in heag2 by co-expressing these domain proteins followed by analysis with native gels and western blotting. We found oligomeric association between these domains. Mutations F30A and A609K (on the surfaces of the PAS and cNBD domains, respectively) affected oligomeric compositions of these domains when proteins for PAS and cNBD domains were expressed together. Taken together, the data suggest that the PAS and cNBD domains form interacting oligomers that have roles in channel function.

Keywords Ion channels · Potassium channels · Electrophysiology · Alanine scanning · Ether-a-go-go channels

L. Stevens · M. Ju · D. Wray (✉)
Faculty of Biological Sciences,
University of Leeds, Leeds LS2 9JT, UK
e-mail: d.wray@leeds.ac.uk

Introduction

Voltage-gated potassium channels play a key role in the function of excitable cells, such as modulating the action potential duration and firing frequency, and setting membrane potentials. These channels are therefore important in the investigation of drug targets and many inherited disorders (Bracey and Wray 2006). Recently, a role for heag1 channels in cancer has been suggested (Pardo and Stuhmer 2008). Many different voltage-gated potassium channels have been characterized and they share a common structure of four α subunits. Each of these subunits contains six membrane-spanning domains (S1–S6), a pore region (P), and intracellular N- and C-terminal domains (Wray 2000; Yellen 2002). The potassium ions pass through a selectivity filter, which is formed from the P region, and the S1–S4 domains form the voltage sensing segment which senses the depolarization of the membrane that causes the channel to open (Yusaf et al. 1996; Gandhi and Isacoff 2002; Bezanilla 2002; Milligan and Wray 2000).

The ether-a-go-go family of voltage-gated potassium channels share this conserved membrane-spanning structure, but also contain an N-terminal 'Per-Ant-Sim' (PAS) domain and a C-terminal cyclic nucleotide binding domain (cNBD) within the long intracellular regions. Although no X-ray structures are available for the PAS and cNBD domains of heag1 and heag2 channels, we have constructed homology models for these domains (Ju and Wray 2006) based on the homologous structures already available for the PAS domain in herg and the cNBD in HCN (Morais Cabral et al. 1998; Zagotta et al. 2003). In the ether-a-go-go channels, most likely just as for HCN channels, the cNBD forms a tetramer hanging below the membrane-spanning part, and is surrounded by the N-terminus (as well as the remainder of the C-terminus).

Within this family, the N-terminal region has been shown to be involved in modulating the channel current (Ju and Wray 2006; Morais Cabral et al. 1998; Chen et al. 1999; Wang et al. 1998; Wang et al. 2000; Schonherr and Heinemann 1996). In particular, for the heag1 and heag2 channels, both the residues at the beginning of the N-terminus and residues within the PAS domain modulate the channel function (Ju and Wray 2006), suggesting interactions with other parts of the channel protein such as the membrane-spanning part or other intracellular regions. For the cNBD domain, no clear role for its effect on channel function has been determined; cyclic nucleotides have little effect on eag channels (Cui et al. 2001), unlike the homologous HCN channels where marked effects of cyclic nucleotides are observed (Zagotta et al. 2003; Craven et al. 2008). In our previous work using chimeras (Ju and Wray 2006), C-terminal regions were swapped between heag1 and heag2 channels without functional effect, which may occur because residues that are conserved between the two isoforms are the important ones in channel function. Many of the conserved residues lie on the surface residues in three-dimensional models of the cNBD domain (Ju and Wray 2006). Such areas of surface residues may form regions of interaction with other domains of the channel, as indeed has already been suggested for the PAS domain in herg (Morais Cabral et al. 1998; Viloria et al. 2000; Gomez-Varela et al. 2002).

In the present study, we have investigated the functional roles of residues predicted in homology models to lie on the surfaces of the PAS and cNBD domains, in order to identify possible distinct areas of interaction between domains. For this, we have made mutations in surface residues of these domains in order to identify the effects of these mutations on heag channel function. We have also investigated the effect of some of these mutations on the oligomeric forms observed on native gels after co-expression of PAS and cNBD proteins.

Materials and methods

Homology models for heag intracellular domains, PAS and cNBD

Homology models (Ju and Wray 2006) were made automatically using Swiss Model (http://swissmodel.expasy.org/SWISS-MODEL.html). Models for the PAS domains in heag1 and heag2 were made based on the crystal structure for the herg PAS domain (PDB ID: 1BYW, Morais Cabral et al. 1998), with 61% homology (32% identity). The model for the heag2 cNBD domain (including the linker to S6) was based on the structures for the HCN2 channel (PDB IDs: 1Q3E and 1Q43, Zagotta et al. 2003), with 42% homology (22% identity); the heag1 cNBD structure was based on the heag2 cNBD structure with 98% homology (91% identity). Tetrameric forms of the cNBD domain were constructed by four-fold symmetry.

Preparation of mutants for electrophysiology

Human cDNA clones in pGEM-HE used in this investigation were heag1 (accession number AJ001366) (Occhiodoro et al. 1998) and heag2 (accession number AF472412, polymorph 2233A) (Ju and Wray 2002). The alanine and lysine mutants in heag1 were generated by a PCR method (QuikChange, Stratagene) using *Pfu Turbo* DNA polymerase (Promega), together with appropriate mutagenic primers. Twenty five cycles were carried out, each cycle consisting of 30 s at 95°C, 1 min at 55°C, and 2 min/kb at 68°C. Products were then digested with *Dpn*I (Promega). All mutants were confirmed by dideoxy sequencing (CoGenics). Linearisation using *Not*I (Promega) was carried out, and capped cRNA was transcribed in vitro using the T7 promoter (Ambion).

Preparation of constructs for native gels

A PAS domain construct of the heag2 channel (residues 25–134) was first sub-cloned in-frame into the pET Duet-1 vector (Novagen). For this, a corresponding PCR product was obtained using sense and anti-sense primers with *Bam*HI and *Not*I overhangs, respectively, and sub-cloned into the His-tagged region of the vector using these enzymes (Promega). Next, a cNBD domain construct of the heag2 channel (residues 550–676) was sub-cloned in-frame into the pET Duet-1 vector containing the PAS domain. This was carried out by first obtaining a cNBD PCR product using sense and anti-sense primers with *Nde*I and *Xho*I overhangs, respectively, and then sub-cloned into the S-tagged region of the vector using these enzymes (Promega). Alanine and lysine mutants in heag2 PAS and cNBD domains (in the Duet vector) were generated as above.

In vitro expression and analysis of PAS and cNBD proteins

The PAS/cNBD co-expression construct in the Duet vector was transformed into One Shot BL21 Star (DE3) *Escherichia coli* cells (Invitrogen). Large scale cultures were grown for 5 h, induced with 0.25 mM isopropyl-1-thio-β-D-galactopyranoside followed by 90 min incubation at 37°C. Cells were then lysed by repetitive freeze/thaw, and the soluble protein fraction separated from the insoluble material by centrifugation. The samples were subjected to 10% SDS-PAGE and verified using western blotting with a

mouse anti-His primary antibody detecting the PAS domain (2 µg/ml, Novagen), or anti-S conjugate primary antibody detecting the cNBD domain (2 µg/ml, Novagen). Detection was with goat anti-mouse secondary antibody (1 µg/ml, Novagen) and horse radish peroxidase enhanced with SuperSignal HRP substrate (Novagen), and ECL detection on film.

Total protein concentration was determined using a Bradford assay (Sigma), and samples were diluted to a total protein concentration of 200 ng/ml and subjected to 12% Tris–glycine gel under native conditions. The composition of the native samples was probed using western blotting with mouse anti-His primary antibody and anti-S conjugated antibody as described above.

Electrophysiology

Xenopus laevis oocytes were prepared and injected with RNA for heag1 wild type or mutant (7 ng in 50 nl). Oocytes were then incubated for 2 days in a modified Barth's solution containing 88 mM NaCl, 1 mM KCl, 2.4 mM $NaHCO_3$, 0.82 mM $MgSO_4$, 0.4 mM $Ca(NO_3)_2$, 7.5 mM Tris–HCl (pH 7.6), penicillin (100 U/l) and streptomycin (1 mg/l) Currents were recorded using two-electrode voltage clamping as previously described (Ju et al. 2003), with sampling rate at 10 kHz and filtering at 5 kHz. Oocytes were held in a 50 µl chamber and continuously perfused with a Ringer's solution containing 2 mM KCl, 115 mM NaCl, 10 mM HEPES, and 1.8 mM $CaCl_2$, at pH 7.2, 22–24°C. To obtain current-voltage (IV) relationships, 500 ms depolarising pulses at a frequency of 0.1 Hz were applied from a holding potential of −80 mV in 10 mV increments from −70 up to 70 mV. All currents were leak subtracted; for this, mean values of twenty 10 mV hyperpolarising steps were taken and then used to calculate the leak current at each test potential. Activation times, $t_{20–80\%}$, were taken as the time for currents to rise from 20 to 80% of maximum current. The Student's *t* test was used to test for statistical significance with significance level set at $P < 0.05$.

Results

Characterisation of the cNBD domain mutants

To explore the functional role of residues located on the surface of the heag cNBD domain, as guided by our homology model, we used site directed mutagenesis to introduce alanine mutations into the channel (or lysine mutations where the native residue was alanine). We started by choosing at random a few conserved residues for mutation located on the surface of the cNBD domain. Then, we carried out experiments on these few initial mutations, and, where there was an observed functional effect, we chose further surface residues for mutation around the affected residue. We then continued this process until we had

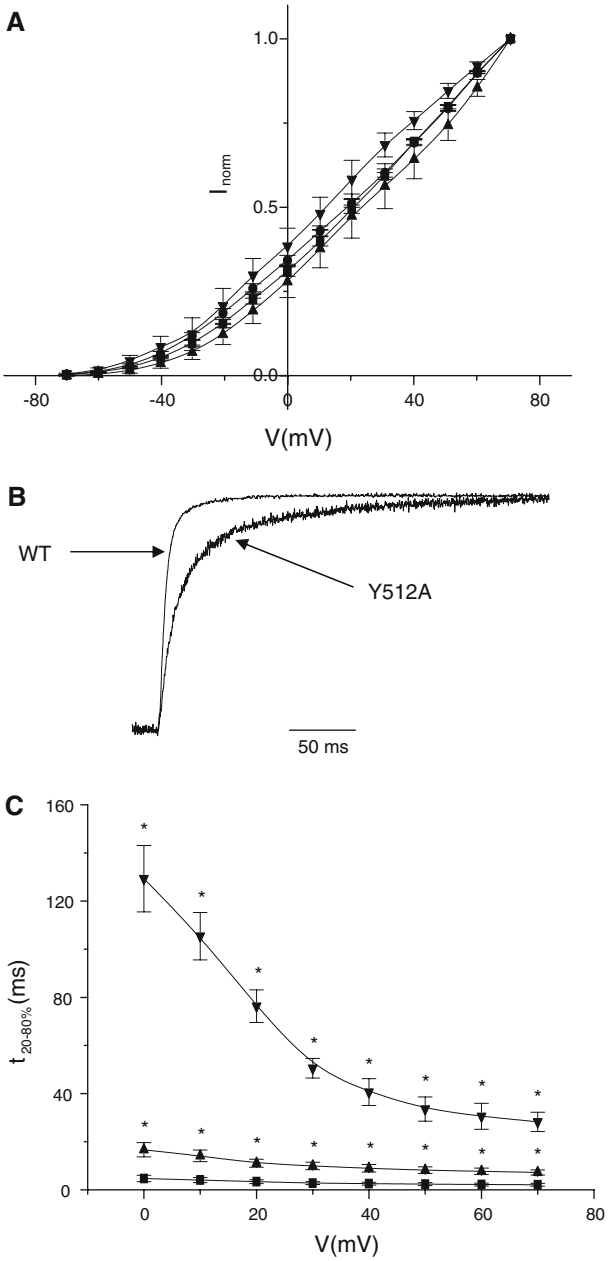

Fig. 1 Currents and activation times for heag1 wild type and alanine mutants. Examples of current-voltage (IV) curves are shown in (**a**) for heag1 wild type channel (*filled circle* $n = 142$), S596A (*filled square* $n = 8$), Y499A (*filled triangle* $n = 12$), T638A (*filled inverted triangle* $n = 8$), normalised to current values at +70 mV. *Smooth curves* are shown through the data points. Example current traces are shown in (**b**) for wild type heag1 and mutant Y512A for steps from −80 to 0 mV, normalised to the same maximum current (*horizontal bar* 50 ms). The activation time (measured as 20–80% maximum, $t_{20–80\%}$) is shown in (**c**) at different test potentials (*V*) for heag1 wild type (*filled square* $n = 142$), Y499A (*filled triangle* $n = 12$), and Y512A (*filled inverted triangle* $n = 10$). *Asterisk* significant differences from wild type currents

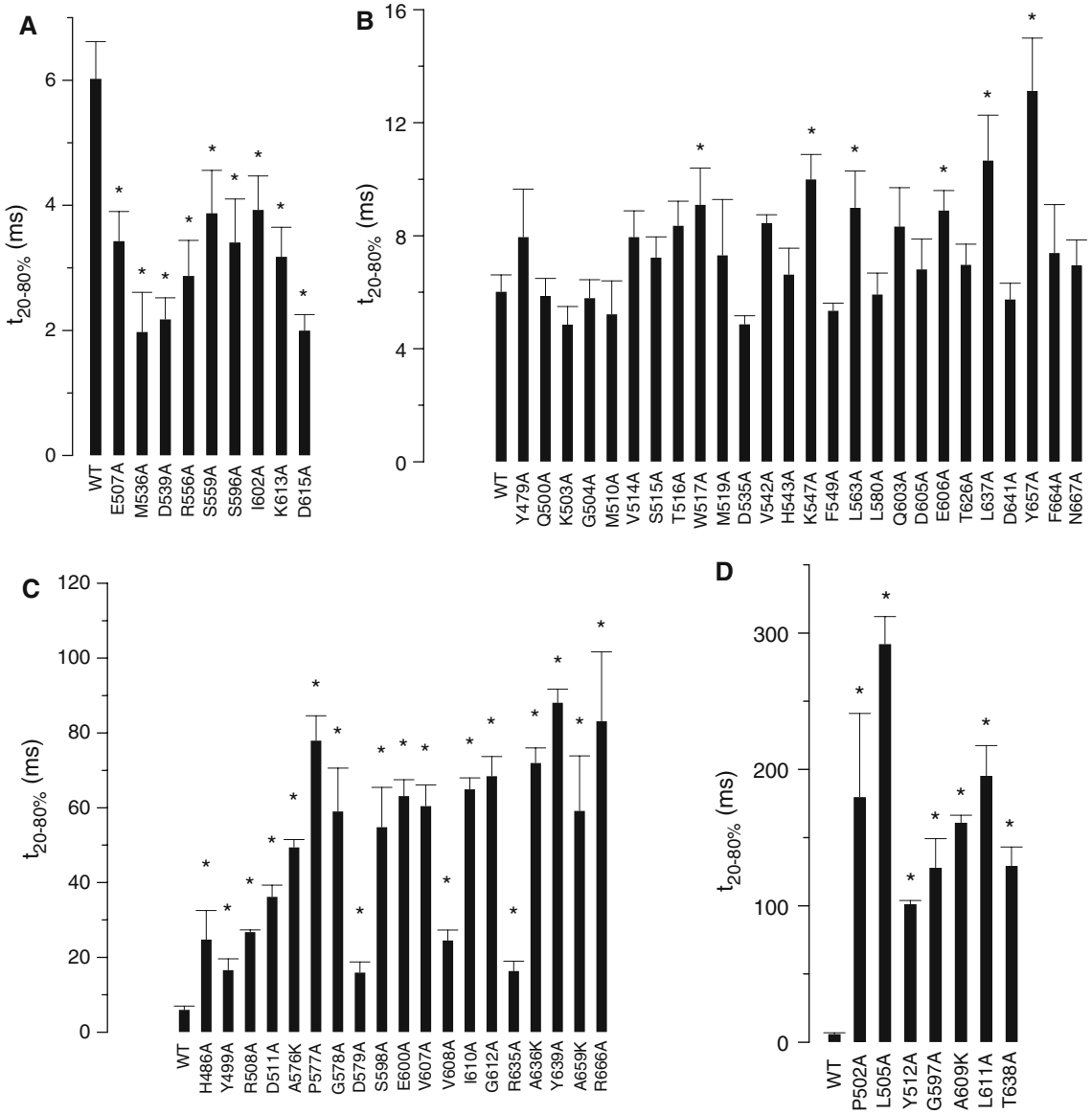

Fig. 2 Activation times for heag1 cNBD mutants. The activation time, $t_{20–80\%,}$ taken at 0 mV test potential (−80 mV holding potential) for alanine and lysine mutants (n = 6–12 for each mutant) of the cNBD is shown in the figure, as compared with wild type (n = 142). The results have been grouped into those showing faster time course than wild type (**a**), similar time course to wild type (including some that were somewhat slower than wild type) (**b**), moderately slower time course than wild type (**c**), and very slow time course (**d**). *Asterisk* significant difference from wild type currents

defined a contiguous region of surface residues that showed mutational effects, surrounded by residues that had no effect. All mutants were expressed in oocytes followed by two-electrode voltage clamp recording.

The main feature of the currents for the mutant channels was often an effect on channel activation kinetics as compared with wild type (see below). On the other hand, IV curves for the mutants were generally similar to wild type IV curves. Examples of IV curves are shown in Fig. 1a for mutants with fast, slow and very slow activation kinetics; there were no significant differences in normalised currents at each test potential. This was the case for 57 out of 61 mutants studied (only mutants Y512A, L563A, Y657A and R666A affected IV curves, with shifts to the right of 5.7, 4.3, 4.8 and 5.1 mV, respectively). Therefore, we did not pursue detailed analysis of IV curves and we have focused the main attention of this study on the activation kinetics where the main mutational effects were observed.

Figure 1b shows examples of currents for wild type and for a very slowly activating mutation Y512A. Figure 1c shows mean activation times, measured as 20–80% of the maximum, plotted against test potential for wild type channel and for examples of mutations with slow and very slow activation (Y499A and Y512A mutations). All data points

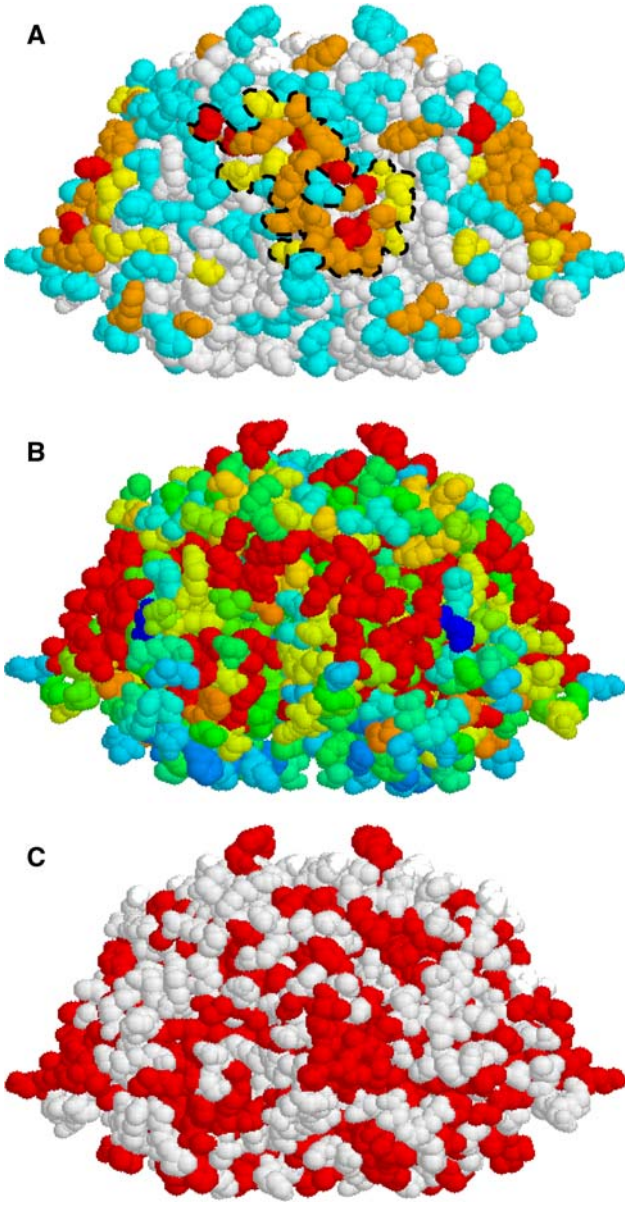

Fig. 3 Surface residues of the heag cNBD domain. *Side views* are shown for the heag cNBD tetramer with space-fill residues, using a homology model (Ju and Wray 2006) based on the HCN cNBD structure (Zagotta et al. 2003). **a** Shows the effects of heag1 mutated residues on activation time (with grouping of residues as in Fig. 2); significantly faster than wild type, *yellow*; similar to wild type, *blue*; moderately slower than wild type, *brown*; much slower than wild type, *red*; not investigated, *white*). In previous work (Ju and Wray 2006), some chimeras with regions swapped between heag1 and heag2 had no effect on activation times, indicating that residues that are different between heag1 and heag2 in such chimeras had no effect on activation; in (**a**), these residues are also shown in *blue*. For clarity, one of the bands of residues that affect activation is shown enclosed by *dashed lines*. Note that the figures shown here are for the tetramer, so that the band occurs four times. **b** Shows the extent of conservation between the eight members of the ether-a-go-go family, with rainbow colours from *red* (100% conservation) to *violet* (17% conservation). **c** Shows the hydrophobic residues (*coloured red*)

for these mutations were significantly different from wild type.

Activation times taken at 0 mV test potential (holding potential −80 mV) are shown in Fig. 2 for all cNBD mutants considered here. As already noted, some of the mutations resulted in activation kinetics that were significantly faster than wild type, some mutations gave similar kinetics to wild type, some were moderately slower, and some were markedly slower. The data for the mutations have been grouped in Fig. 2 according to the effect on activation kinetics (fast, Fig. 2a; no effect or slightly slower, Fig. 2b; moderately slow, Fig. 2c; very slow, Fig. 2d). The position of these residues on the surface of the homology model for the cNBD is shown in Fig. 3a, indicating in different colour the magnitude of the effect on activation (yellow, fast; blue, no effect or slightly slower; brown, moderately slow; red, very slow). It is very striking that most residues that affect activation lie in a band across the side of the cNBD tetramer; these are the red and brown residues shown in Fig. 3a. Interestingly, the majority of the residues in this band are located within a region of a band of conserved residues, as shown in Fig. 3b (rainbow colour coded with red as the most conserved across eight members of the ether-a-go-go family). The fact that there is a surface band of conserved residues that also affect activation is suggestive of a region of interaction of this surface of the cNBD with other domains of the heag channel. This conclusion is also supported by the fact that many of the residues affecting activation also form a hydrophobic band (Fig. 3c).

Characterisation of the PAS domain mutants

To explore the activation properties of individual residues within the heag1 N-terminal PAS region, we again used site directed mutagenesis to introduce alanine mutations (and one lysine mutation). Again, IV curves for the mutants were generally not significantly different from wild type, except for 2 out of 21 mutants studied where shifts to the right were observed (R57A, N118A, with shifts of 5.9 and 4.2 mV, respectively).

As for the cNBD mutants, the main effect of the PAS mutations was on activation kinetics. The activation times at 0 mV test potential are shown in Fig. 4. Results fell into three groups: some mutations gave currents that were similar to wild type currents (Fig. 4a), some showed somewhat slower currents than wild type (Fig. 4b) and some showed markedly slower currents (Fig. 4c). None of the PAS residues mutated caused the activation kinetics to be faster than the wild type. The position of these residues on the surface of the PAS homology model is shown in Fig. 5a, again indicating in different colour the magnitude of the effect on activation (blue, similar to wild type; brown, moderately

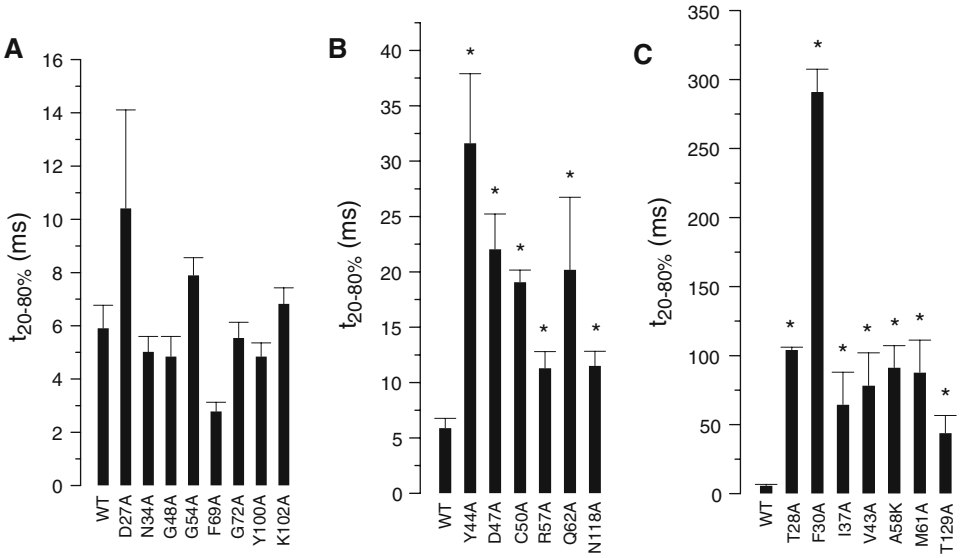

Fig. 4 Activation times for heag1 PAS mutants. The activation time, $t_{20–80\%}$, taken at 0 mV test potential (−80 mV holding potential) for alanine and lysine mutants (n = 6–12 for each mutant) of the PAS domain is shown in the figure, as compared with wild type (n = 142). The results have been grouped into those showing similar time course to wild type (**a**), moderately slower time course than wild type (**b**), and very slow time course (**c**). *Asterisk* significant difference from wild type currents

slower than wild type; red, markedly slower than wild type). Again it is striking that most residues affecting activation lie in a band on the surface of the PAS domain, mostly co-incidental with a corresponding band of conserved residues (Fig. 5b) and some hydrophobic residues (Fig. 5c). This surface band of conserved PAS residues affecting activation is again suggestive of a region of interaction of this surface with other domains of the heag channel.

In vitro characterisation of Heag2 co-expressed protein domains, PAS and cNBD

Since surface residues of both PAS and cNBD domains were found to affect channel function, we have investigated whether oligomeric forms between these two domains can form, and whether surface mutations can affect the ability to form oligomers. For this, the PAS and cNBD domain proteins were co-expressed and then oligomeric forms examined under native conditions. Mutants in the PAS and cNBD domains that were identified above to have a large effect on activation kinetics were chosen for this study.

To first check expression of PAS and cNBD domain proteins, co-expressed proteins were subjected to 10% SDS-PAGE under denaturing conditions (Fig. 6a). When compared to the uninduced protein in lane 1, all of the constructs expressed soluble protein of the correct size, although PAS and cNBD bands cannot be distinguished by size (14.8 kDa for PAS, and 13.6 kDa for cNBD). To establish whether both of the domains had been co-expressed, western blots were carried out from the denaturing SDS-PAGE gel using His- and S-tag antibodies. After visualisation using chemiluminescence, it can be seen that both the PAS domain (detected by His-tag antibody, Fig. 6b) and the cNBD domain (detected by S-tag antibody, Fig. 6c) were present in all of the constructs, and the levels of expression were similar. These experiments were repeated nine times with similar results.

The co-expressed PAS and cNBD proteins were then subjected to Tris–glycine gels to determine the oligomeric states under native conditions. When compared to uninduced protein (lane 1, Fig. 7a), strong bands can be seen within the samples for wild type and mutant proteins (lanes 2–5), with a band at 14 kDa for the monomer and additional bands at 27, 57 and 114 kDa, indicating various oligomeric states of the channel PAS/cNBD domain proteins (the origin of the sub-band below 14 kDa is not clear). The pattern of bands seen on the gel is similar for wild type and mutant channels, but there are differences in intensities of the bands. For cNBD mutant A609K there was a marked increase in intensity of the 27 kDa band, and for PAS mutant F30A there was an increase in intensity of the 114 kDa band (Fig. 7a), suggesting that these mutations affect the oligomeric state. These changes in intensity were confirmed by measuring the absorbance for averages of six experiments with co-expression of PAS and cNBD proteins (Fig. 7b).

To determine the composition of PAS and cNBD domain proteins in each band, western blots of the native gels were carried out to detect the presence of His- and S-tags in each of the bands. For the His-tag native western blot (detecting the PAS domain), bands were seen at 114 kDa for the F30A mutant (Table 1), and 57 kDa for all of the mutants (Fig. 7c), indicating the presence of PAS at these sizes. Although the PAS domain protein was not consistently detected at 27 and 14 kDa bands (and wild type at 57 kDa), it is clear from the denatured western blots (described above and carried out in parallel at the same time on the same material) that the PAS domain protein is expressed. The lack of detection in native western blots may be due to the His-tag remaining buried in the native structure, so that the masking of the tag may have

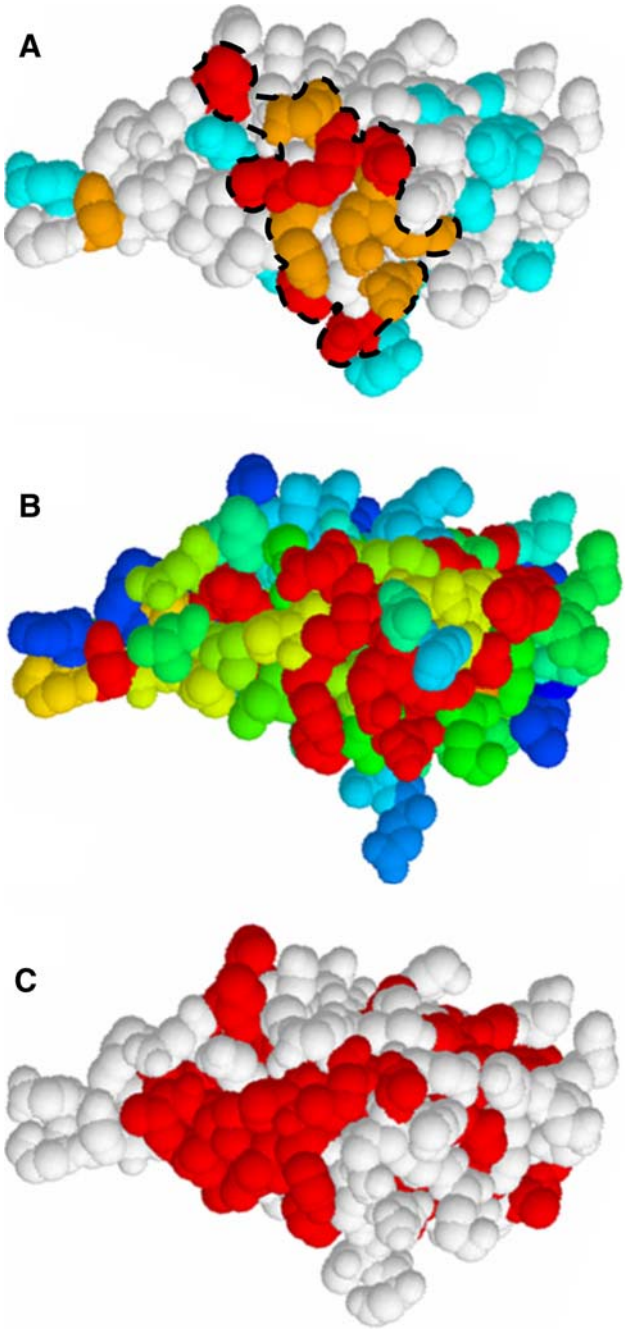

Fig. 5 Surface residues of the heag PAS domain. Views are shown for the heag PAS domain with space-fill residues, using a homology model (Ju and Wray 2006) based on the herg PAS domain (Morais Cabral et al. 1998). **a** Shows the effects of heag1 mutated residues on activation time (with grouping as in Fig. 4), not significantly different from wild type, *blue*; moderately slower than wild type, *brown*; much slower than wild type, *red*; not investigated, *white*). As for Fig. 3 data for residues in heag1/heag2 chimeras with no effect on $t_{20-80\%}$ are also shown in *blue*. For clarity, the band of residues that affect activation is shown enclosed by *dashed lines*. The figures shown here are for the PAS monomer. **b** Shows the extent of conservation between the eight members of the ether-a-go-go family, with rainbow colours from *red* (100% conservation) to *violet* (17% conservation). **c** Shows the hydrophobic residues (*coloured red*)

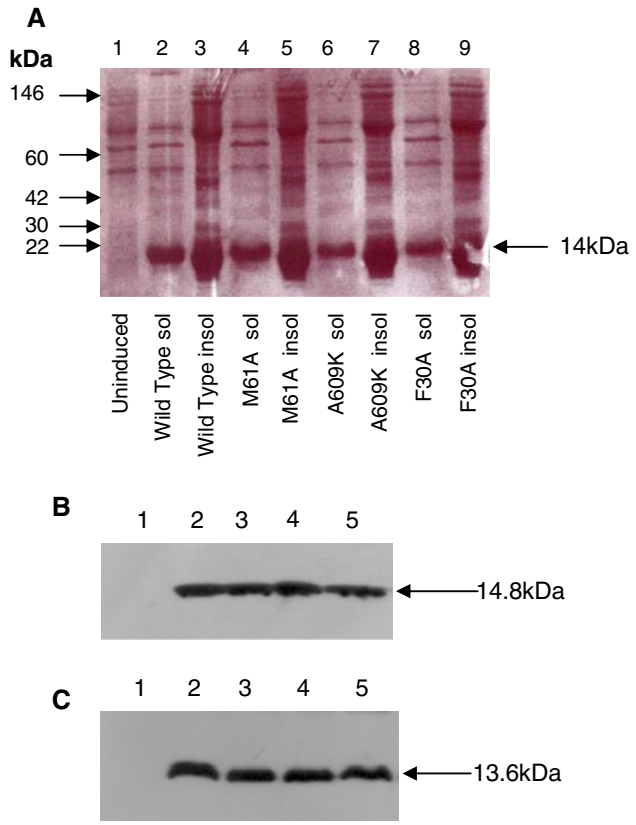

Fig. 6 Denaturing SDS-PAGE gel of the cNBD and PAS co-expressed heag2 proteins. The PAS and cNBD proteins were co-expressed in *E. coli*, and **a** shows the soluble and insoluble fractions, resolved by denatured SDS-PAGE visualised with Coomassie blue. Examples are shown for the wild type, M61A, A609K, and F30A mutations. An *arrow* indicates the correct size of 14 kDa for the co-expressed cNBD and PAS domain proteins (14.8 kDa for the PAS and 13.6 kDa for the cNBD domain). A denaturing western blot using anti-His-tag antibody is shown in (**b**), detecting the PAS domain, with lanes corresponding to un-induced protein *lane 1*, wild type *lane 2*, M61A *lane 3*, A609K *lane 4*, and F30A *lane 5*. A denaturing western blot using anti-S-tag antibody is shown in (**c**) detecting the cNBD, with lanes as in (**b**)

prevented detection. For the S-tag native western blot (detecting the cNBD domain), in most cases, bands were observed at 14, 27 and 57 kDa, and at 114 kDa for the F30A mutant protein (Fig. 7d; Table 1). For the 14 and 27 kDa bands, only the cNBD protein was detected (Table 1), but as mentioned above, the PAS domain may have escaped detection; thus the composition of these bands as monomer and dimer are difficult to interpret. Results for six co-expressions are summarized in Table 1. The data show that both PAS and cNBD proteins are present at 57 and 114 kDa bands, suggesting perhaps the possible presence of a 2:2 complex or 4:4 complex of the PAS and cNBD domains, respectively, in these bands (Table 1).

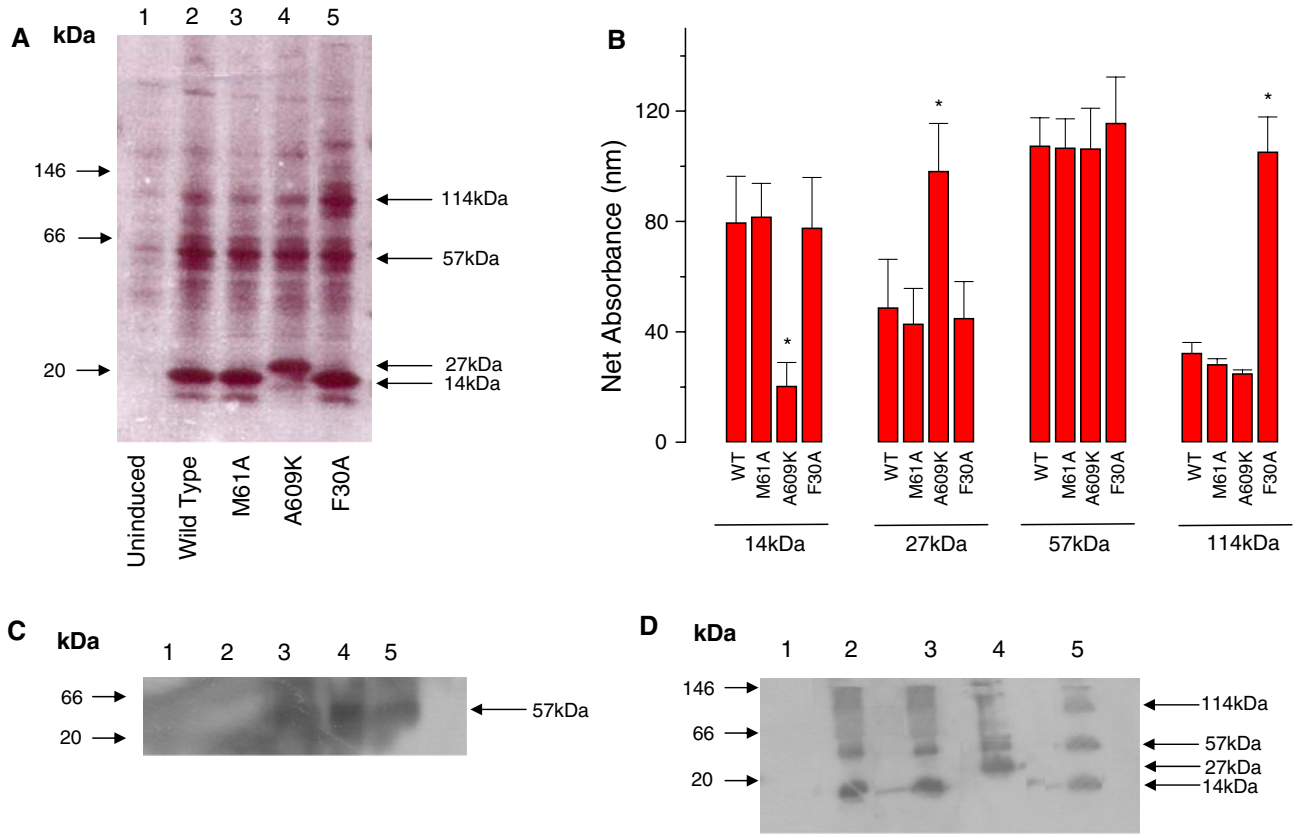

Fig. 7 Native gel analysis of the cNBD and PAS co-expressed heag2 protein. The PAS and cNBD proteins were co-expressed in *E. coli*, and (**a**) shows the soluble fraction, resolved by native Tris–glycine gel, visualised with Coomassie blue. Examples are shown for the wild type, M61A, A609K, and F30A mutants. *Arrows* indicate the strong bands at 14, 27, 57, and 114 kDa, which correspond to various oligomeric states of the channel. For six such gels, mean values of absorbance of these bands is shown in (**b**). The background absorbance of uninduced protein has been subtracted from the wild type and mutant values in all cases. A native western blot using anti-His-tag antibody is shown in (**c**) for the uninduced protein, wild type, M61A, A609K, and F30A mutants (*lanes 1–5*, respectively). Although the background is high using this His-tag detection system (see "Methods"), bands can be discerned at 57 kDa for the mutants. A native western blot using anti-S-tag antibody is shown in (**d**), with lanes corresponding to uninduced protein, wild type, M61A, A609K, and F30A mutants (*lanes 1–5*, respectively), with bands indicated by the *arrows*. *Asterisk* significant difference from heag2 wild type

Table 1 Western blot detection of bands in native gels

kDa	Uninduced	WT	M61A	A609K	F30A	Oligomer
114	None	None	None	None	cNBD (6); PAS (5)	$(CP)_4$
57	None	cNBD (6)	cNBD (6); PAS (5)	cNBD (6); PAS (5)	cNBD (6); PAS (5)	$(CP)_2$
27	None	cNBD (1)	cNBD (1)	cNBD (6)	cNBD (1)	$(C)_2$, CP?
14	None	cNBD (5)	cNBD (5)	cNBD (1)	cNBD (5)	C, P?

The table shows a summary of the bands found in native western blots at the sizes indicated for mutants and wild type, in experiments with co-expression of PAS and cNBD domains, with detection by His-tag and S-tag, respectively. The experiment was repeated six times, and the numbers in brackets show the numbers of times the respective bands were obtained. In the column headed "Oligomer", the suggested oligomeric forms of the expressed domains in each band are shown (*C*, cNBD domain; *P*, PAS domain)

However, both PAS and cNBD proteins were detected only for mutant F30A at 114 kDa. Thus, it may be that this mutation strengthens the oligomeric structure; mutational effects on activation kinetics in principle may act either by strengthening or weakening possible interactions between subunits. For the bands at 27 and 14 kDa, where no PAS domain protein was detected in native westerns (Table 1), interpretation of the bands is more difficult and may comprise combinations of cNBD and PAS, or cNBD alone.

These results taken together indicate that the mutants M61A, A609K and F30A all affect the oligomeric compositions of the native proteins when compared to wild type, and also seem to affect the accessibility of antibodies to detect the tags.

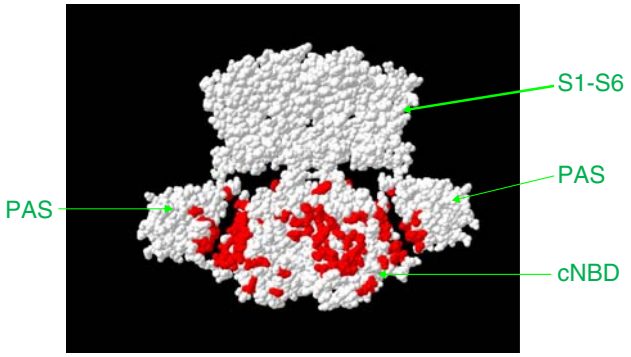

Fig. 8 Possible localisation of heag2 PAS and cNBD domains. The figure shows how the intracellular domains PAS and cNBD may assemble, and their possible relation to the membrane-spanning part of the channel. The homology model for the tetrameric cNBD domain is shown hanging below the membrane-spanning part of the channel, surrounded by two PAS domains on either side. Only two of the four PAS domains are shown for clarity. The bands of residues coloured *red* are those affecting activation time, and the orientation between the PAS and cNBD domains has been positioned by eye so that these bands lie next to each other. The membrane-spanning part has simply been added for illustration and orientation purposes and comprises the KvAP structure for S1–S4 and KcsA for S5–S6 (Lee et al. 2005; Jiang et al. 2002). The PAS-to-S1 linker and the C-terminal region after the cNBD are not shown, as no models are available

Discussion

In this study, we have investigated the structural and functional role of residues located on the surfaces of the PAS and cNBD domains in heag potassium channels. Using scanning mutagenesis studies, we have shown that, on the surface of both the PAS and cNBD domains in the three-dimensional structures, there are bands of residues that contribute to determining the activation kinetics of the channel. These surface bands of residues correspond to bands of conserved residues within the ether-a-go-go family, as well as including many hydrophobic residues, suggestive of regions of domain–domain interaction via these surfaces within the complete channel structure. In studies using co-expressed PAS and cNBD proteins and native gels, we have shown the existence of various oligomeric forms of these domains. Furthermore, mutation of some surface residues of these domains that affected activation also affected the relative distribution of oligomers in native gels. An interesting finding is that mutations that slow activation potentially may enhance formation of multimeric complexes; this raises the interesting possibility that stronger binding between domains of the channel might somehow make the channel protein more rigid and less able to undergo conformational change.

Our data shows that mutations in the conserved surface regions affected both channel function and oligomeric forms of the PAS/cNBD domains, pointing towards an interaction between these domains. It would indeed be very interesting in future work to study direct binding interaction using tagged domains. If the domains indeed interact, it is likely that the PAS domains then lie at the sides of the tetrameric cNBD, the structures hanging together below the membrane, as suggested in Fig. 8. In this figure, the PAS domains have been depicted to lie in positions such that the bands of residues affecting activation kinetics lie in overlapping interfaces. The concept of an N-terminal domain interacting with a C-terminal domain is consistent with a general picture for other ion channels in different families where N- and C-terminal domains interact and affect function, such as in the Kv (Ju et al. 2003; Mohapatra et al. 2008; Scholle et al. 2004) and Kir families (Jones et al. 2001). Clearly, it would be very useful in future studies to carry out biochemical studies in vitro to directly investigate binding between the PAS and cNBD domains using tagged constructs. It could of course be argued that our use of a bacterial expression system may lead to complexes in vitro that do not represent complexes formed in intact channels.

In previous work on the herg channel, a hydrophobic region on the PAS domain was identified that was suggested to interface with the main body of the channel (Morais Cabral et al. 1998). This conclusion was based on similar arguments to our own regarding effects of bands of surface mutations on function, and also by rescue of PAS-deleted channel function by the addition of the PAS protein. However, for the herg PAS domain, extensive scanning mutagenesis was not carried out, and so far only two surface residues have been found to have an effect on functional properties (deactivation) (Morais Cabral et al. 1998); indeed the latter residues in herg also slowed activation in heag (residues F30 and Y44, Fig. 4b, c). Our data extends and supports the concept of interaction, and clarifies further the surface regions of interaction for both PAS and cNBD domains.

The molecular regions of heag1 and heag2 have been systematically studied in a chimeric approach to determine the importance of regions affecting the activation kinetics (Ju and Wray 2006). It was found that the extreme N-terminus (residues 1–27 of heag2), the PAS domain, and multiple regions of the membrane-spanning domain are all involved in determining activation kinetics. The heag1/heag2 chimeric study (Ju and Wray 2006) did not find a role of the C-terminus in determining activation properties. However, as mentioned in the "Introduction", the chimeric study is only sensitive to changes in amino acids between heag1 and heag2, so that conserved residues were not probed. Indeed, in the present study, we have shown that C-terminal residues that are conserved between heag1 and heag2 play a role in activation properties. It is the very good conservation of residues within the family that most likely underlies a common structural orientation and architecture of domains within the channels of this family.

Regarding the site of interaction of the PAS domain with the rest of the channel protein, besides interacting with the

cNBD as we have suggested, there are also possible functional interactions with the membrane-spanning part (Ju and Wray 2006; Lorinczi et al. 2008; Terlau et al. 1997), which may occur if the PAS domain is located at the side of the cNBD just below the membrane, as in Fig. 8. Indeed, interactions have been reported between the N-terminus and the S4/S5 linker for members of the ether-a-go-go family, although interactions usually reported with S4/S5 are with the extreme N-terminus rather than with the PAS domain itself (Terlau et al. 1997).

In summary, our results show that bands of conserved residues on the surfaces of both the N-terminal PAS domain and the C-terminal cNBD domain are important in determining the activation kinetics of heag potassium channels. Mutation of some of these residues affected the oligomeric state of these intracellular domains. Taken together, the data indicate important functional and structural interactions between intracellular domains of the channel.

Acknowledgments This research was supported by the Biotechnology and Biological Sciences Research Council (Grant Ref; BB/C004922/1). Construction of the tetrameric cNBD model from the single homology model subunit was made by S.E.V. Phillips and C. Trinh; the model for relative orientations of subunits was by D. Elliott.

References

Bezanilla F (2002) Voltage sensor movements. J Gen Physiol 120:465–473. doi:10.1085/jgp.20028660

Bracey K, Wray D (2006) Inherited disorders of ion channels. In: Voltage gated ion channels as drug targets, Wiley, NY

Chen J, Zou A, Splawski I, Keating MT, Sanguinetti MC (1999) Long QT syndrome-associated mutations in the Per-Arnt-Sim (PAS) domain of HERG potassium channels accelerate channel deactivation. J Biol Chem 274:10113–10118. doi:10.1074/jbc.274.15.10113

Craven KB, Olivier NB, Zagotta WN (2008) C-terminal movement during gating in cyclic nucleotide-modulated channels. J Biol Chem 283:14728–14738. doi:10.1074/jbc.M710463200

Cui J, Kagan A, Qin D, Mathew J, Melman YF, McDonald TV (2001) Analysis of the cyclic nucleotide binding domain of the HERG potassium channel and interactions with KCNE2. J Biol Chem 276:17244–17251. doi:10.1074/jbc.M010904200

Gandhi CS, Isacoff EY (2002) Molecular models of voltage sensing. J Gen Physiol 120:455–463. doi:10.1085/jgp.20028678

Gomez-Varela D, de la Pena P, Garcia J, Giraldez T, Barros F (2002) Influence of amino-terminal structures on kinetic transitions between several closed and open states in human erg K^+ channels. J Membr Biol 187:117–133. doi:10.1007/s00232-001-0156-4

Jiang Y, Lee A, Chen J, Cadene M, Chalt BT, MacKinnon R (2002) The open pore conformation of potassium channels. Nature 417:523–526. doi:10.1038/417523a

Jones PA, Tucker SJ, Ashcroft FM (2001) Multiple sites of interaction between the intracellular domains of an inwardly rectifying potassium channel, Kir6.2. FEBS Lett 508:85–89. doi:10.1016/S0014-5793(01)03023-X

Ju M, Wray D (2002) Molecular identification and characterisation of the human eag2 potassium channel. FEBS Lett 524:204–210. doi:10.1016/S0014-5793(02)03055-7

Ju M, Wray D (2006) Molecular regions responsible for differences in activation between heag channels. Biochem Biophys Res Commun 342:1088–1097. doi:10.1016/j.bbrc.2006.02.062

Ju M, Stevens L, Leadbitter E, Wray D (2003) The roles of N- and C-terminal determinants in the activation of the Kv2.1 potassium channel. J Biol Chem 278:12769–12778. doi:10.1074/jbc.M212973200

Lee SY, Lee A, Chen J, MacKinnon R (2005) Structure of KvAP voltage-dependent K^+ channel and its dependence on the lipid membrane. Proc Natl Acad Sci USA 102:15441–15446. doi:10.1073/pnas.0507651102

Lorinczi E, Napp J, Contretas-Jurado C, Pardo LA, Stuhmer W (2008) The voltage dependence of hEag currents is not determined solely by membrane-spanning domains. Eur Biophys J. doi:10.1007/s00249-008-0319-7

Milligan CJ, Wray D (2000) Local movement in the S2 region of the voltage-gated potassium channel hKv2.1 studied using cysteine mutagenesis. Biophys J 78:1852–1861

Mohapatra DP, Siino DF, Trimmer JS (2008) Interdomain cytoplasmic interactions govern the intracellular trafficking, gating, and modulation of the Kv2.1 channel. J Neurosci 28:4982–4994. doi:10.1523/JNEUROSCI.0186-08.2008

Morais Cabral JH, Lee SL, Cohen BT, Chait BT, Li M, Mackinnon R (1998) Crystal structure and functional analysis of the HERG potassium channel N terminus: a eukaryotic PAS domain. Cell 95:649–655. doi:10.1016/S0092-8674(00)81635-9

Occhiodoro T, Bernheim L, Liu JH, Bijlenga P, Sinnreich CR, Bader CR, Fischer-Lougheed J (1998) Cloning of a human ether-a-go-go potassium channel expressed in myoblasts at the onset of fusion. FEBS Lett 434:177–182. doi:10.1016/S0014-5793 (98)00973-9

Pardo LA, Stuhmer W (2008) Eag1: an emerging oncological target. Cancer Res 68:1611–1613. doi:10.1158/0008-5472.CAN-07-5710

Scholle A, Zimmer T, Koopmann R, Engeland B, Pongs O, Benndorf K (2004) Effects of Kv1.2 intracellular regions on activation of Kv2.1 channels. Biophys J 87:873–882. doi:10.1529/biophysj.104.040550

Schonherr R, Heinemann SH (1996) Molecular determinants for activation and inactivation of HERG, a human inward rectifier potassium channel. J Physiol 493:635–642

Terlau H, Heinemann SH, Stuhmer W, Pongs O, Ludwig J (1997) Amino terminal-dependent gating of the potassium channel rat eag is compensated by a mutation in the S4 segment. J Physiol 502:537–543. doi:10.1111/j.1469-7793.1997.537bj.x

Viloria CG, Barros F, Giraldez T, Gomez-Varela D, de la Pena P (2000) Differential effects of amino-terminal distal and proximal domains in the regulation of human erg K(+) channel gating. Biophys J 79:231–246

Wang J, Trudeau MC, Zappia AM, Robertson GA (1998) Regulation of deactivation by an amino terminal domain in human ether-à-go-go-related gene potassium channels. J Gen Physiol 112:637–647. doi:10.1085/jgp.112.5.637

Wang J, Myers CD, Robertson GA (2000) Dynamic control of deactivation gating by a soluble amino-terminal domain in HERG K(+) channels. J Gen Physiol 115:749–758. doi:10.1085/jgp.115.6.749

Wray D (2000) Ion channels: molecular machines par excellence. Sci Spectr 23:64–71

Yellen G (2002) The voltage-gated potassium channels and their relatives. Nature 419:35–42. doi:10.1038/nature00978

Yusaf SP, Wray D, Sivaprasadarao A (1996) Measurement of the movement of the S4 segment during the activation of a voltage-gated potassium channel. Eur J Phys 433:91–97. doi:10.1007/s004240050253

Zagotta WN, Olivier NB, Black KD, Young EC, Olson R, Gouaux E (2003) Structural basis for modulation and agonist specificity of HCN pacemaker channels. Nature 425:200–205. doi:10.1038/nature01922